Proceedings of the ASME 2022 41th International Conference on Ocean, Offshore and Arctic Engineering, OMAE2022
June 5 - 10, 2022, Hamburg, Germany

OMAE2022-81467

IDENTIFICATION OF WAVE DRIFT FORCES ON A FLOATING WIND TURBINE SUB-STRUCTURE WITH HEAVE PLATES AND COMPARISON WITH PREDICTIONS

Nuno Fonseca SINTEF Ocean Trondheim, Norway nuno.fonseca@sintef.no	**Synne Nybø** SINTEF Ocean Trondheim, Norway synne.nybo@sintef.no	**José Miguel Rodrigues** SINTEF Ocean Trondheim, Norway miguel.rodrigues@sintef.no
Aitor Gallego SAITEC Spain aitorgallego@saitec.es	**Carlos Garrido** SAITEC Spain carlosgarrido@saitec.es	

ABSTRACT

The paper presents empirical quadratic transfer functions (QTFs) of the horizontal wave drift loads on a turret moored floating wind turbine in operational and in severe sea states. Comparison between the empirical results and potential flow predictions of mean wave drift coefficients provide an assessment of the limitations of state of the art numerical tools.

The floating substructure has a catamaran configuration with heave plates to minimize the vertical motions. The empirical QTFs are determined from cross bi-spectral analysis of model test data obtained in an ocean basin. Validation of the identified QTFs is provided by comparing low frequency motions reconstructed from the empirical QTF with measurements. The comparisons are performed in terms of low frequency spectra and motion time histories.

The numerical mean wave drift coefficients are calculated by a panel code that solves the wave-structure linear potential flow problem. Systematic comparisons between numerical predictions and empirical QTFs allows identification of tendencies of the empirical QTFs and limitations of the potential flow predictions, namely with respect to the sea state severity and with respect to wave-current interaction effects. The results indicate a decrease of the wave drift coefficients with increasing sea state severity. Furthermore, wave-current effects for collinear conditions increase the empirical wave drift coefficients.

INTRODUCTION

Mooring analysis for floating structures requires a correct prediction of floater motions induced by environmental loads. If the motions are accurate, as compared to model test data for example, then the mooring line tensions are correctly calculated by cable dynamic tools, such as based on finite element methods [1]. Regarding prediction of the vessel motions, estimation of low frequency (LF) horizontal motions induced by second order wave drift loads is particularly challenging and relevant. While prediction of LF motions is reasonably accurate for small sea states, there is a significant uncertainty related to estimations in moderate and severe sea states. Furthermore, the LF horizontal motions may be one order of magnitude larger than the corresponding wave frequency motions, therefore they contribute strongly to the mooring line tensions.

Recent experience shows that state of the art radiation/diffraction codes tend to underestimate the wave drift loads in moderate and severe sea states for conventional semi-submersibles and mono-hull such as FPSOs (Floating, production, storage and offloading vessel). Therefore, the mooring line tensions are underestimated as well. For column stabilized units, viscous wave drift is acknowledged to contribute to the wave drift loads if the wave height is large enough ([2], [3], [4]). Similar conclusions have been presented for a floating wind turbine (FWT) semi-submersible sub-structure with three columns [5]. Such effects are not considered by potential flow codes. Underprediction of wave drift loads in severe sea states

by potential flow codes has been observed for FPSOs as well [1], [6].

Some studies have been reported on the low frequency motions induced by wave drift forces on floating wind turbines. Lopez-Pavon [7] analysed results from captive model tests with a three-column semi-submersible FWT. Comparisons with numerical QTFs and with Newman's approximation [8] lead to the conclusion that full QTFs are needed to correctly represent the wave drift loads for the difference frequency representing the assumed surge natural period (58 s). Simos et al. [9] extended the previous study for the moving platform, therefore the model tests were performed with a moored model of the FWT. The observations were consistent with the previous study: full QTFs were needed for correct prediction of wave drift forces and Newman's approximation is unconservative in this case.

Additional studies reporting underpredictions of low frequency surge and pitch of floating wind turbines have been presented in the scope of the OC phases 5 and 6 [10], [11] (OC – offshore code comparison collaboration) and by Azcona et al. [12].

The sub-structure of the FWT considered herein is different from the other cases investigated before, both within offshore wind sector and the oil and gas sector. It is a twin-hull structure, with large submerged heave plates, moored at a single point (more details in the following Section). For this reason, it is of interest to assess the hydrodynamic behaviour of this novel design in terms of wave drift forces. The study is based on model test data obtained in an Ocean basin in the scope of the MooringSense EU financed research and innovation project. The measured motion results in small, moderate and severe sea states are post-processed with a second order signal analysis technique, known as cross bi-spectral analysis, to identify empirical (pseudo) QTFs of the surge wave drift forces. Assessment of results for different sea states indicates significant variation of the QTF with respect to the sea state severity and to the current effects. Comparison with results from a potential flow code based on the panel method leads to conclusions with regard to the limitations of state of the art hydrodynamic numerical tools commonly used for mooring analysis.

THE MOORINGSENSE PROJECT

MooringSense is a collaborative research and innovation project finance by the EU as part of the HORIZON 2020 work programme. The objective is to develop efficient strategies and tools for mooring system integrity management of floating wind turbines (FWT), including sensing technology. The results will reduce operational costs and increase annual energy production.

A digital twin (DT), or virtual replica, of the mooring system is an important component of the MooringSense concept and it consists of information and numerical tools. These tools are based on a fully coupled numerical model of the FWT, or they use results from this numerical model. The six tools have the following functionalities:

- Virtual measurements of mooring line loads.
- Continuous calculation of synthetic rope properties.
- Prediction of floater motions.
- Calculation of remaining lifetime.
- Mooring re-analysis
- Calculation of local damages in chains.

The MooringSense reference case is based on the SATH sub-structure concept by SAITEC which supports a 10 MW wind turbine. It consists of a twin hull platform with cylindrical floaters. Heave plates minimize the wave induced vertical motions. Station keeping is achieved with a single point mooring system, which allows the platform to weathervane with respect to the environmental loads. The mooring system is designed for 120 m water depth, and it includes six lines composed of a bottom chain segment, an intermediate polyester segment and an upper chain segment.

Figure 1 shows the sub-structure and Figure 2 the mooring system. Table 1 presents the main properties of the FWT and mooring system.

Figure 1. SATH concept by SAITEC.

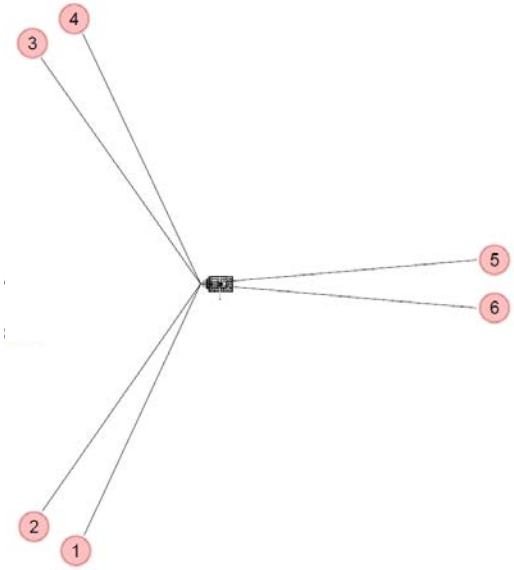

Figure 2. Turret moored system.

Table 1. Main properties of the SATH FWT.

Parameter	Value	Unit
Wind turbine capacity	10	MW
Length	104.2	m
Beam (width)	47.5	m
Hub height	108	m
Draft	9.4	m

MODEL TESTS

Between September and October 2021, tests were carried out with a scaled down physical model of the MooringSense Floating Wind Turbine in the Ocean Basin at SINTEF Ocean (SATH concept by SAITEC). A Froude scaling of 1:36 was used for the tests with a full-scale water depth of 120 m.

The test campaign was performed to acquire data to assess, tune, and validate the MooringSense numerical models and concepts. Specifically, the empirical data set will allow to:

- Validate the concept of virtual measurement of mooring line tensions.
- Calibrate and validate the coupled numerical model for the FWT dynamics, namely the hydrodynamic models for wave-structure interactions and models for the global coupled responses (mooring dynamics – hull hydrodynamics – wind induced responses – servo control).
- Assess the performance of the models for monitoring the mooring system structural integrity to identify degraded conditions.

The test matrix includes tests with waves only, waves and current, and wave and wind. For the tests with wind, the wind turbine rotor and tower loads were applied by use of the Real-Time Hybrid Model test method [14], [15]. A small sea state, with waves from 0 and 20 degrees, is represented by a broad banded wave spectrum (pink-noise spectrum Test 3011 and 3020). Pink noise sea states are useful for identification of linear response amplitude operator of the floater responses and quadratic transfer function for wave drift loads. Operational- and severe sea states with waves from 0 and 20 degrees are represented by a JONSWAP wave spectrum. Some sea states were repeated for several different realizations (different seeds) to reduce the sample variability of the hydrodynamic properties to be identified. The tests' duration was 3 hours and 20 minutes at full scale. The initial 20 minutes were discharged before the time signals were post-processed to remove transient effects.

The work presented here-in is focusing on the investigation of hydrodynamic wave-structure interaction, specifically on the low frequency wave excitation. For this reason, only the tests in waves and in waves and current are considered here. Table 2 presents the test matrix for conditions with waves only and waves and current only (Hs, Tp, Gamma and Uc stand for significant wave height, wave peak period, peakedness parameter, and current velocity).

Instrumentation was used to measure:

- Wave elevation at 3 positions in the ocean basin during calibration. Two of the sensors were kept during the tests.
- Current velocity during calibration.
- The platform motions in 6 degrees of freedom.
- Relative wave elevation at 5 locations.
- Accelerations at the platform and at the nacelle.
- Angular velocities at the nacelle.
- Mooring line tensions at fairlead (6 lines).
- Hydrodynamic pressure at the heave plates at 16 positions.
- Tensions at the 5 cable-driven robots (wind loads by the Real-Time Hybrid Model Test method).

Table 2. Tests in waves and waves and current.

Test no.	Test type	Hs [m]	Tp [s]	Gamma	seed	Uc [m/s]	Head. [deg]
3011	PINK	3	4.5-20	-	1	0	0
3020	PINK	3	4.5-20	-	1	0	20
3040	IRR	2.5	7.5	1.34	1	0	0
3050	IRR	4.5	9.5	1.82	1	0	0
3060	IRR	8	10	5.00	1	0	0
3110	IRR	1.5	5.5	3.30	1	0.5	0
3120	IRR	2.5	7.5	1.34	1	0.5	0
3130	IRR	2.5	7.5	1.34	2	0.5	0
3140	IRR	2.5	7.5	1.34	3	0.5	0
3150	IRR	2.5	7.5	1.34	4	0.5	0
3160	IRR	2.5	7.5	1.34	5	0.5	0
3170	IRR	1.5	5.5	3.30	1	0.5	20
3180	IRR	4.5	9.5	1.82	1	0.5	0
3210	IRR	4.8	7.5	5.00	1	1.2	0
3220	IRR	8	10	5.00	1	1.2	0
3230	IRR	8	10	5.00	2	1.2	0
3240	IRR	8	10	5.00	3	1.2	0
3250	IRR	8	10	5.00	4	1.2	0
3260	IRR	8	10	5.00	5	1.2	0
3272	IRR	8	10	5.00	1	1.2	20
3280	IRR	10.5	14.3	1.96	1	1.2	0

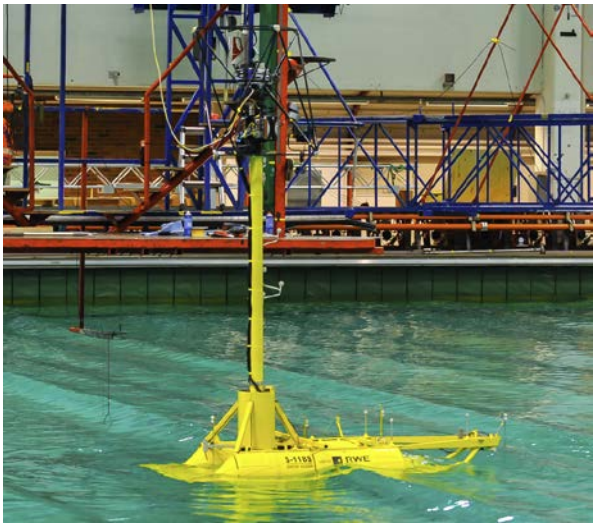

Figure 3. MooringSense SATH FWT during tests.

IDENTIFICATION OF EMPIRICAL QTFs

Cross bi-spectral analysis

A method is followed in the present study to estimate realistic quadratic transfer functions (QTFs) of wave drift forces for the MooringSense platform. A post-processing analysis of the test data is carried out to extract empirical “wave drift coefficients” making use of a nonlinear data analysis method known as "cross-

bi-spectral analysis" to estimate characteristics of second-order (quadratic) responses [13], [3].

The procedure starts by identifying the second order wave force signal from the measured motion responses; second, it uses the incident wave elevation and the estimated 2nd order force, together with cross bi-spectral analysis, to identify the empirical QTFs.

It is assumed that the floater motion induced by irregular waves is represented by an expansion:

$$x(t) = x^{(0)} + x^{(1)}(t) + x^{(2)}(t) + E_x(t) \qquad (1)$$

where $x^{(0)}$ represents a mean offset, $x^{(1)}(t)$ is the linear component of the motion, $x^{(2)}(t)$ is the second order motion component and $E_x(t)$ represent higher order effects.

We neglect sum frequency effects as well as higher order effects, therefore a low pass filter is applied to $x(t)$ to remove the wave frequency response (and any higher harmonics). The mean offset is removed as well, so that the resulting signal represents the slow drift oscillations $x^{(2)}(t)$.

The next step assumes the low frequency horizontal motions are decoupled, so that they may be represented by a one degree of freedom oscillator. The dynamic equation of motion is:

$$\ddot{x}(t) + 2\xi\omega_n\dot{x}(t) + \omega_n^2 x(t) = \frac{1}{m} g^{(2)}(t) \qquad (2)$$

where $\xi = c/2m\omega_n$, c and m are the system damping factor (or damping ratio), damping coefficient and mass, $\omega_n = 2\pi f_n$, f_n is the natural frequency in Hz and $g^{(2)}$ is the 2nd order difference frequency wave exciting force. ω_n and m are known from the model tests, while ξ is estimated iteratively (further details ahead in the text), which allows an identification of $g^{(2)}(t)$.

The wave exciting forces are represented by an expansion similar to (1):

$$g(t) = g^{(0)} + g^{(1)}(t) + g^{(2)}(t) + E_g(t) \qquad (3)$$

where $g^{(0)}$ is the mean wave drift force, $g^{(1)}(t)$ is the force response component linear with respect to the undisturbed incident wave elevation $z\,(t)$ and it may be expressed as function of the complex Fourier transform of $z\,(t)$ and of the complex linear force transfer function, namely $Z(f)$ and $H^{(1)}(f)$:

$$g^{(1)}(t) = \int_{-\infty}^{\infty}\left[Z(f)H^{(1)}(f)e^{i2\pi ft}\right]df \qquad (4)$$

One assumes the wave elevation follows a Gaussian distributed process with zero mean.

The second term of expansion (2), $g^{(2)}(t)$, represents the quadratic component, which can be represented by:

$$g^{(2)}(t) = \int_{-\infty}^{\infty}\int_{-\infty}^{\infty}\left[Z^*(f_m)Z(f_n)H^{(2)}(f_m,f_n)e^{i2\pi(f_m-f_n)t}\right]df_m df_n \qquad (5)$$

where $H^{(2)}(f_m, f_n)$ is the complex wave force quadratic transfer function (QTF).

The Fourier transform of $g^{(2)}(t)$ gives:

$$G^{(2)}(f) = \int_{-\infty}^{\infty}\left[g^{(2)}(t)e^{-i2\pi ft}\right]dt\,, \quad f = (f_m - f_n) \qquad (6)$$

Cross bi-spectral analysis is applied to estimate the QTF. The cross bi-spectrum of $g^{(2)}(t)$ with respect to $z\,(t)$ is given by:

$$S_{\zeta\zeta g}(f_m, f_n) = < Z^*(f_m)Z(f_n)G^{(2)}(f_m - f_n) > \qquad (7)$$

where < > means statistical averaging.

Combining equations (5), (6) and (7) leads to an expression for estimation of the QTF (see Stansberg, 1997):

$$H^{(2)}(f_m, f_n) = S_{\zeta\zeta g}(f_m, f_n)/S_{\zeta\zeta}(f_m)S_{\zeta\zeta}(f_n) \qquad (8)$$

where $S_{\zeta\zeta}(f)$ is the wave spectrum.

The main difficulty in applying the cross bi-spectral analysis is related to the statistical averaging in equation (7). Stansberg [13] discusses further this aspect, where a noise reduction method based on imaging processing principles was introduced.

Example

The following paragraphs present an example of results from the cross bi-spectral analysis for a long crested sea state with Hs = 2.5 m and Tp = 7.5 s, test 3040. The wave heading is 0 degrees and there is no current.

Figure 4 shows the estimated surge difference frequency wave exciting force QTF. The bi-frequency plane axes are in Hz and the colours represent the wave drift coefficients magnitude in kN/m^2. Dashed white lines follow diagonals with constant difference frequency of 0.00897 Hz, which corresponds to the surge natural frequency.

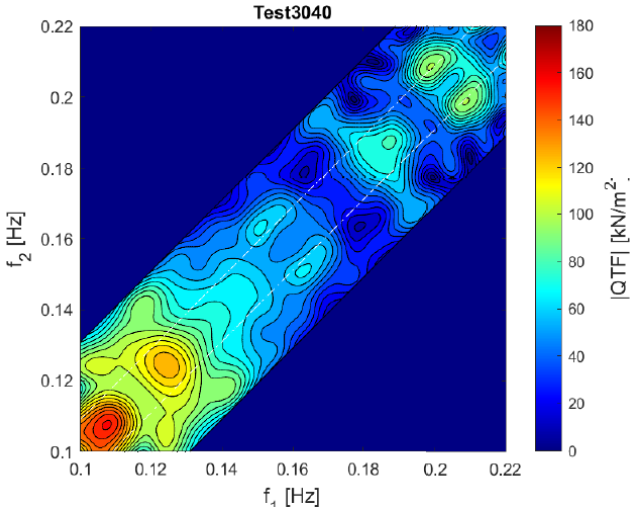

Figure 4. Empirical surge QTF: heading = 0 deg., Hs = 2.5 m, Tp = 7.5 s, Uc = 0. Horizontal axes with frequency in Hz and wave drift coefficients in kN/m^2.

Comparison between the measured low frequency motion and the low frequency motion reconstructed from the empirical QTF solving equation 2 provides an assessment of the quality of the identified QTF. The comparison is performed for the time histories and the low frequency spectra. An example is presented in Figure 5 and Figure 6 for the same sea state. The response

spectrum is normalized by the significant wave height and the natural period (Tn) in surge ($Hs^2 * Tn$) and the frequency axis by the natural frequency (fn). The agreement between measured and reconstructed signals is very good, which validates the procedure to identify the wave drift coefficients.

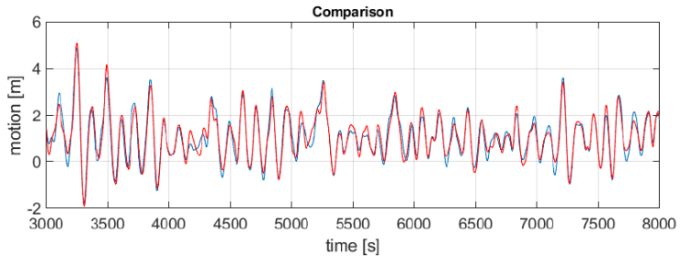

Figure 5. Comparison between measured slow drift surge motion (blue line) and reconstructed from the identified empirical QTF (red line).

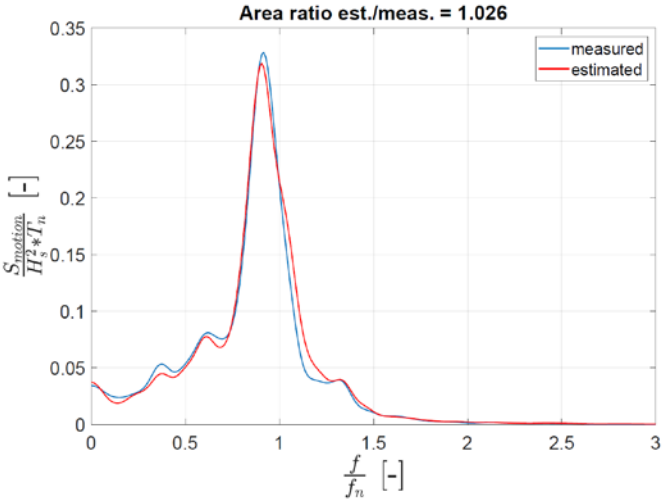

Figure 6. Spectra of low frequency surge motion. Comparison between experimental motion (blue) and motion reconstructed from the identified QTF (red).

POTENTIAL FLOW RADIATION/DIFFRACTION MODEL

The potential flow calculations are performed with WAMIT®. The code is based on the boundary element method, and it solves the wave-structure first order radiation/diffraction problems. The numerical solution is established by discretizing the mean hull wetted surface and the heave plates into a finite number of flat panels, namely 3791 and 1340 panels respectively for half body. Advantage is taken of the vessel plane of symmetry for the hydrodynamic calculations therefore only half body is needed. The heave plates are represented by zero thickness elements, or dipoles.

Additional stiffness coefficients in surge and sway represent the mooring system effects. Additional damping coefficients are applied in all modes of motion to represent linearized viscous damping effects and in this way limit the RAOs resonant peaks to realistic values. This is important since the wave drift force coefficients depend on the wave frequency motions, therefore the level of damping will affect the wave drift force prediction, especially around the motion resonance frequencies. The additional damping coefficients were tuned to achieve a good match between predicted and measured motion transfer function resonance peaks for moderate sea states.

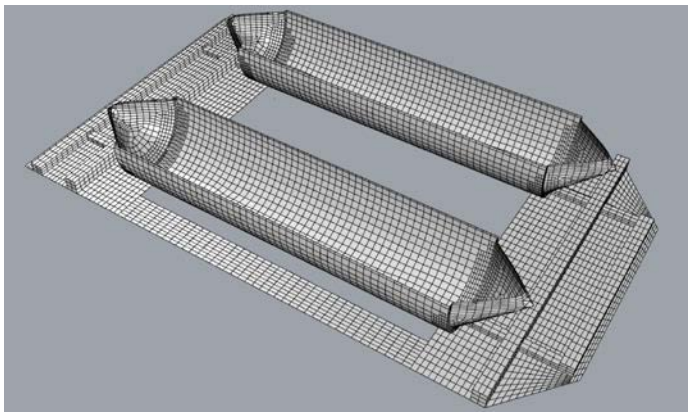

Figure 7. MooringSense sub-structure wetted body and heave plates mesh for potential flow calculations.

RESULTS

Results for the surge wave drift force QTF in head sea obtained by cross bi-spectral analysis are presented for small, moderate and severe sea states. The sea states include conditions with and without current. The current is collinear with the waves. The empirical QTFs from different sea states are compared to mean wave drift components obtained by potential flow theory. In addition, empirical surge wave drift load spectra are compared for different sea states with and without current. The results emphasise the dependence of the QTFs on the sea state characteristics, the effects of wave-current interaction and the limitations of potential flow predictions.

One should note that the cross bi-spectral analysis applied herein to identify QTFs from model test data have some inherent uncertainty, or sample variability, related to the finite duration of the experimental time series. We use effective records with three hours duration full scale, which results in about 100 low frequency surge cycles. For this reason, both the QTFs and the drift load force spectra presented in the following paragraphs show some random oscillations.

Furthermore, the identification procedure provides estimates of wave drift coefficients within the frequency range where the waves have energy. As an example, Figure 8 presents four diagonals of empirical QTF from test 3060 (blue lines) within the nondimensional frequency range of 1.6 to 2.7. This is the frequency range where the related wave spectrum has most of the energy, as seen also in the plot. The uncertainty in the identification increases at low and high frequencies where there is little wave energy.

Finally, since the identification is based on the measured low frequency motions, the procedure identifies a limited difference frequency band around the QTF main diagonal. There are no

harmonic components in the low frequency motion signal with a difference frequency larger than a certain value.

The aspects discussed in the previous paragraphs are not really limitations of the method, since the QTF is identified within the wave frequency and difference frequency ranges of interest for the particular sea state, meaning that QTF coefficients outside these ranges do not contribute to the vessel low frequency motions.

Effect of sea state severity

Figure 8 shows a comparison between empirical wave drift coefficients and the potential flow mean wave drift coefficients, with focus on the effect of increasing sea state. The empirical coefficients correspond to three tests without current: the pink noise small sea state (3011), a moderate sea state (3050) and a severe sea state (3060). See Table 2 for the properties of the different sea states.

The empirical coefficients correspond to four diagonals of the QTF with difference frequencies (df) distributed between 0 and the surge natural frequency (fn). The non-dimensional constants in the axes titles are L, a characteristic length, g, the acceleration of gravity, ρ, the fluid specific mass density and ζ, the wave amplitude.

Two features stand out from the plot of Figure 8:

- The reduction of the wave drift force coefficients as the sea state severity increases.
- The large overestimation of potential flow predictions around the first peak of the numerical curve (around the nondimensional frequency of 1.9).

Furthermore, the empirical results corresponding to the small sea state (3011) seem to agree well with the potential flow predictions for low and high frequencies, meaning below 1.7 and above 2.5.

Figure 9 presents similar results to Figure 8, however in this case for sea states with collinear waves and current of 0.5 m/s. Test 3120 corresponds to a small sea state (red lines) and test 3180 to a moderate sea state (green lines). We observe, again, a reduction of the wave drift coefficients with the increase of the sea state, a very significant one in this case.

The reduction of wave drift force coefficients with increasing sea state and the overestimation by potential flow predictions is surprising. It is the opposite of previous observations for semi-submersibles and monohull – see the brief review presented in the Introduction. Further investigations are needed to determine the root causes for the behaviour empirical QTFs. The hypothesis is that the large heave plates introduce drag effects, and possibly lift effects, that contribute to the low frequency surge motions. Such effects are not represented by standard potential flow numerical tools.

The other relevant observation from Figure 9 is the large underestimation of drift forces from the potential flow predictions for the small sea state with current. The following Section discusses wave-current effects on the drift forces.

Effect of wave-current interaction

Several of the tested conditions repeat the same sea state without current and with current. By "same sea state" we mean that the waves were calibrated to achieve the same target wave spectrum, therefore not only the *Hs* and *Tp* are the same without and with current, but also the spectral shape is nearly the same. For conditions with current, the wave and the current propagate in the same direction. These tests provide a good basis to assess the influence of wave-current effects on the wave drift forces.

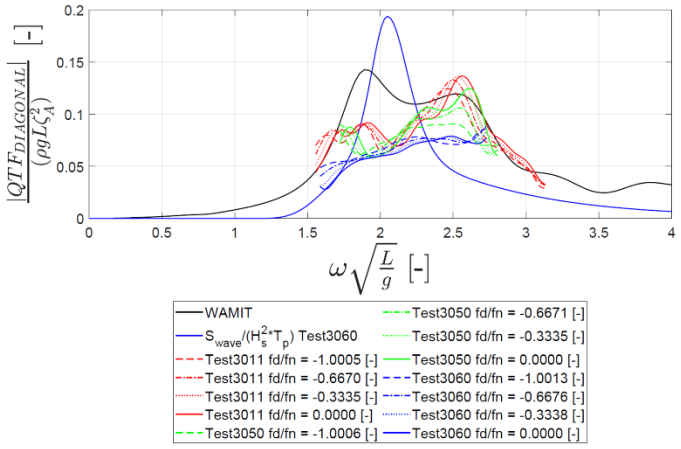

Figure 8. Effect of sea state severity without current. Comparison between potential flow mean wave drift coefficients (WAMIT) and empirical wave drift coefficients from a pink noise sea state (test 3011), a moderate and a severe sea state (tests 3050 and 3060).

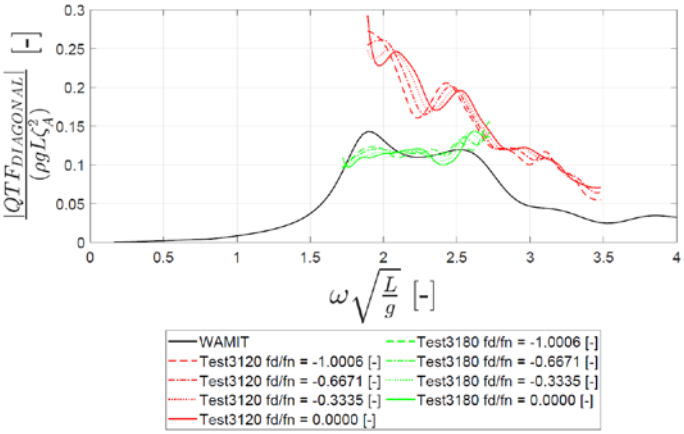

Figure 9. Effect of sea state severity with current. Comparison between potential flow mean wave drift coefficients (WAMIT) and empirical wave drift coefficients from a small sea state (test3120) and a moderate sea state (test 3180).

Figure 10 and Figure 11 show the empirical surge wave drift QTF modulus for two small sea states, the first without current and the second with a 0.5 m/s current. The second QTF corresponds to an average of five QTFs identified for the same sea state and five different realizations of the wave elevation. The aim is to obtain an empirical QTF with lower uncertainty, or sample variability. The thin white dashed lines in the plots

represent the diagonals with difference frequency equal to the surge natural frequency.

The plots show a large increase of the QTF amplitude for the sea state with current, especially for frequencies below around 0.16 Hz. The increase is observed for all diagonals of the QTF.

Comparing wave drift force spectra for the same sea state without and with current is also a good way of illustrating the wave-current effects on the wave drift forces. Figure 12 presents the wave drift load spectra for a small sea state without current (test 3040) and with current (test 3120, Uc = 0.5 m/s). The results are normalized by *Hs* squared, therefore, for sea states with the same *Tp*, the drift force spectra should be similar (expect for the random variations). The results corresponding to the conditions with current show larger wave drift forces along the whole low frequency range.

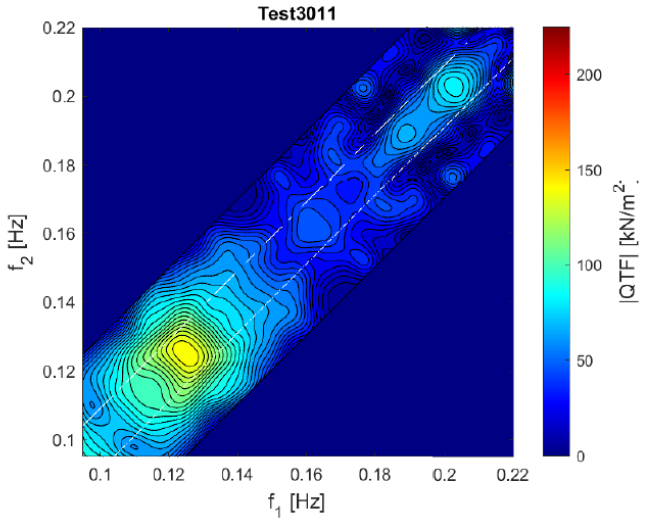

Figure 10. Surge wave drift force QTF modulus. Hs = 3.0 m, Tp = 4.5-20s s, Uc = 0 m/s (pink noise test 3011).

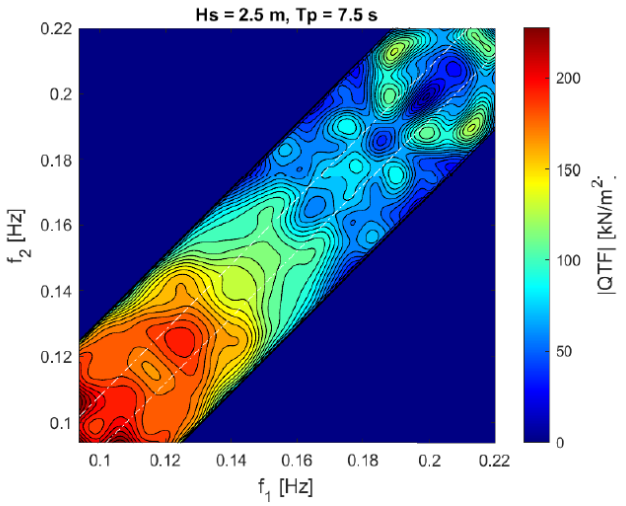

Figure 11. Surge wave drift force QTF modulus. Hs = 2.5 m, Tp = 7.5 s, Uc = 0.5 m/s (average QTF from test 3120, 3130, 3140, 3150 and 3160).

Figure 13 presents similar results, in this case for a larger sea state and higher current velocity (1.2 m/s). The observation is the same, although the differences between conditions without and with current are smaller compared to the lower sea state.

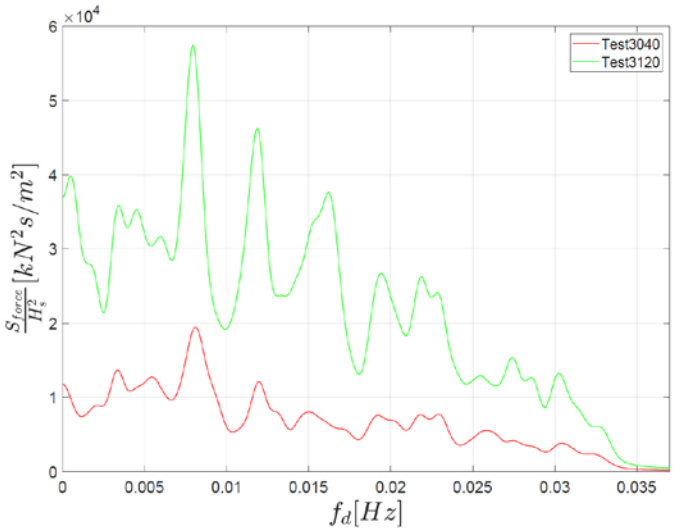

Figure 12. Comparison of empirical surge drift force response spectra for a small sea state, Hs = 2.5 m, Tp = 7.5 s, without current (test 3040) and with current Uc = 0.5 m/s (test 3120).

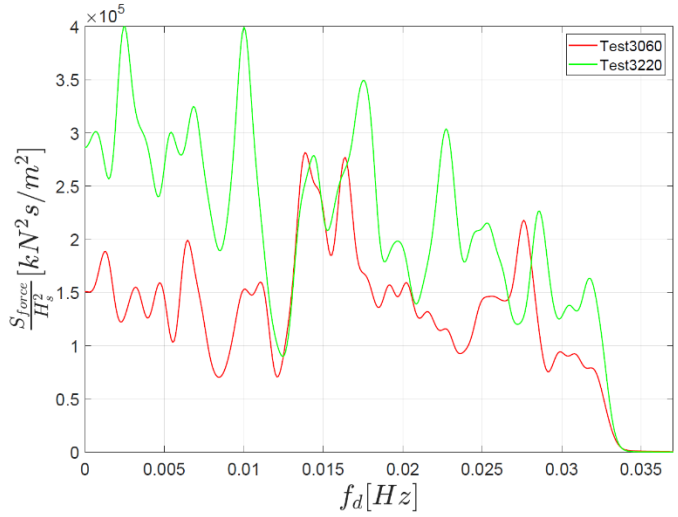

Figure 13. Comparison of empirical surge drift force spectra for a severe sea state, Hs = 8.0 m, Tp = 10.0 s, without current (test 3060) and with current Uc = 1.2 m/s (test 3220).

Empirical QTFs for the cases discussed in the previous paragraphs are shown is Figure 14 and Figure 15. Figure 14 corresponds to the small sea state. The empirical results for conditions without current compare quite well with the potential flow results. We have noted before in the text that overprediction occurs around the nondimensional frequency of 1.9, where the present sea state has little energy and identification is not

possible. On the other hand, the same sea state with current results in larger wave drift coefficients.

The same conclusion is taken from the plot of Figure 15 with the results for the severe sea state. The interesting observation is that the relative difference between drift coefficients without and with current is smaller than the small sea state case, even if the current velocity is higher in the former (1.2 m/s compared to 0.5 m/s). The reason is not known, but it might be related to complex viscous effects on the heave plates which affect the wave drift loads differently in small and large sea states.

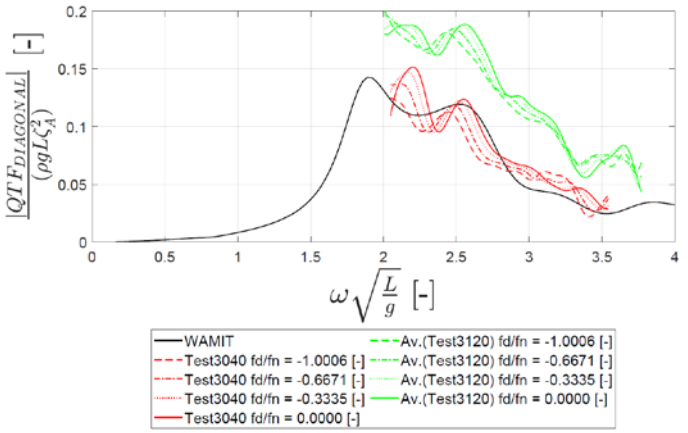

Figure 14. Effect of current for a small sea state (Hs = 2.5 m, Tp = 7.5 s). Comparison between potential flow mean wave drift coefficients (WAMIT) and empirical coefficients from test 3040 without current and average from tests 3120 to 3160 with current Uc = 0.5 m/s.

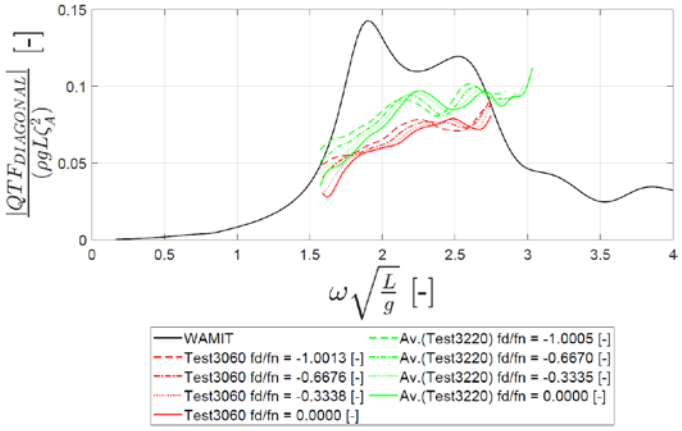

Figure 15. Effect of current for a severe sea state (Hs = 8.0 m, Tp = 10.0 s). Comparison between potential flow mean wave drift coefficients (WAMIT) and empirical coefficients from test 3060 without current and average from tests 3220 to 3250 with current Uc = 1.2 m/s.

CONCLUSIONS

The paper presents a systematic study of model test data applying a second order signal analysis method to identify (pseudo) quadratic transfer functions (QTFs) of the surge wave drift forces on a floating wind turbine sub-structure. The result is named "pseudo" because it varies significantly with the sea state.

It is concluded that the wave drift force coefficients reduce as the severity of the sea state increases. This feature is observed for conditions both without current and with current. This is a surprising conclusion, since previous observations for semi-submersibles and monohulls are exactly opposite. While the root causes are still not known, the hypothesis is that the large heave plates introduce drag effects, and possibly lift effects, that contribute to the low frequency surge motions. Such effects are not represented by standard potential flow numerical tools.

One second observation is the overprediction by the potential flow tool, even in small sea states, for a frequency band around the peak of the potential flow wave drift curve. Since the wave drift coefficients decrease with the severity of the sea state, the actual wave drift forces are significantly lower than potential flow predictions for moderate and severe sea states. The SATH concept has quite favourable hydrodynamic properties also in this respect.

Wave-current effects, for waves and current propagating in the same direction, increase the wave drift forces. The relative influence is larger for small sea states than for high sea states. Given the differences observed for the same sea states without and with current, wave-current effects should not be neglected in a mooring analysis.

The low frequency motions are proportional to the wave drift loads. In fact, there is a linear relation in case the damping and the mooring restoring are linear. Due to the properties of relatively shallow water depth (120 m), the line tensions are quite nonlinear therefore it is expected that line tensions increase at a steeper rate than the motions. For this reason, it is expected that the observed differences between predicted and identified wave drift forces, which are not small, will drive to larger differences on the mooring line tensions. These aspects will be further investigated.

ACKNOWLEDGEMENTS

The work was developed within the MooringSense project, which received funding from the European Union's Horizon 2020 research and innovation programme under grant agreement No 851703.

REFERENCES

[1] Aksnes, V.Ø., Berthelsen, P.A., Fonseca, N., Reinholdtsen, S-A, 2015. On the need for calibration of numerical models of large floating units against experimental data. *The 25th International Offshore and Polar Engineering Conference*, Kona, Hawaii Big Island, USA, June 21-26.

[2] Dev, A.K. and Pinkster, J.A., 1994, "Experimental evaluation of the viscous contribution to mean drift forces on vertical cylinders. *Proceedings 7th International Conference on the Behaviour of Offshore Structures*

(BOSS'94), Massachusetts Institute of Technology, Editor C. Chyssostomidis, Elsevier, **2**, pp. 855 - 875.

[3] Stansberg, C.T. 2001, "Data Interpretation and System Identification in Hydrodynamic Model Testing", *Proc of 11th Int. Offshore and Polar Eng. Conf., ISOPE,* Stavanger, Norway.

[4] Fonseca, N., Stansberg, C.T., Larsen, K., Bjørkly, R., Vigesdal, T. and Dalane, O., 2021. Low frequency wave loads and damping of four MODUs in severe seastates with current. *Journal* of Offshore Mechanics and Arctic Engineering, 143 (1).

[5] Fonseca, N., Thys, M., Berthelsen, P.A., 2021. Identification of wave drift force QTFs for the INO WINDMOOR floating wind turbine based on model test data and comparison with potential flow predictions. *Journal of Physics*: Conference Series, 2018 012017.

[6] Fonseca, N. and Stansberg, C.T., 2017. Wave drift forces and low frequency damping on the Exwave FPSO. *Proc. of the ASME 2017 36th Int. Conf. on Ocean, Offshore and Arctic Eng.*, June 25-30, 2017, Trondheim, Norway, paper OMAE2017-62540.

[7] Simos, A.N., Ruggeri, F., Watai, R.A., Souto-Iglesias, A., 2018. Slow-drift of a floating wind turbine: An assessment of frequency domain methods based on model tests. *Renewable Energy*, vol. 116, part A, pp. 133-154.

[8] Newman, J.N., "Second-Order, Slowly Varying Forces on Vessels in Irregular Waves", *Proc., Int. Symp. On Dynamics of Marine Vehicles and Structures in Waves*, London, UK, 1974.

[9] Lopez-Pavon, C., Watai, R.A., Ruggeri, F, Simos, A.N., Souto-Iglesias, A., 2015. Influence of wave induced second order forces in semisubmersible FOWT mooring design. *Journal of Offshore Mechanics and Arctic Engineering*, vol. 137.

[10] Robertson, A., et al., 2017. OC5 Project Phase II: Validation of global loads of the DeepCwind floating semisubmersible wind turbine, *Energy Procedia*, 137, pp. 38-57.

[11] Robertson, A.N., et al., 2020. OC6 Phase I: Investigating the under-prediction of lowfrequency hydrodynamic loads and responses of a floating wind turbine. *J. Phys.: Conf. Ser. 1618* (TORQUE 2020).

[12] Azcona, J., Bouchotrouch, F., and Vittori, F., 2019. Low-frequency dynamics of a floating wind turbine in wave tank–scaled experiments with SiL hybrid method. *Wind Energy*, 22, pp. 1402-1413.

[13] Stansberg, C.T., 1997. Linear and nonlinear system identification in model testing. *International Conference on Nonlinear Aspects of Physical Model Tests*, OTRC, Texas A&M University, College Station, Texas, 2-3 May 1997.

[14] Sauder, T., Chabaud, V., Thys, M., Bachynski, E. E., and Sæther, L. O., 2016, Real-Time Hybrid Model Testing of a Braceless Semi-Submersible Wind Turbine: Part I — The Hybrid Approach, Volume 6: Ocean Space Utilization; Ocean Renewable Energy, ASME, Busan, South Korea.

[15] Thys, M., Chabaud, V., Sauder, T., and Eliassen, L., 2018, "Real-Time Hybrid Model Testing of a Semi-Submersible 10MW Floating Wind Turbine and Advances in the Test Method," Proceedings of the ASME 2018 1st International Offshore Wind Technical Conference, ASME, San Francisco, California, USA, p. 11.

